PAPER

Check for updates

NMR-based quantitative studies of the conformational equilibrium between their square and folded forms of ascidiacyclamide and its analogues†

Akiko Asano, [ID] * Katsuhiko Minoura, Yuki Kojima, Taishi Yoshii, Ryoya Ito, Takeshi Yamada, [ID] Takuma Kato [ID] and Mitsunobu Doi [ID]

Ascidiacyclamide [cyclo(-Ile^{1,5}-oxazoline^{2,6}-D-Val^{3,7}-thiazole^{4,8}-)] (**1**) is a cytotoxic cyclic peptide from the ascidian, or sea squirt. Through structural analyses using asymmetric analogues [Xxx^1: Ala (**2**), Val (**3**), Leu (**4**), Phe (**5**), cyclohexylalanine (**6**) and phenylglycine (**7**)], we previously showed **1** to exist in a conformational equilibrium between square and folded forms. In the present study, five new asymmetric analogues [Xxx^1: 2-aminobutyric acid (**8**), 2-aminopentyric acid (**9**), *tert*-butylalanine (**10**), cyclohexylglycine (**11**) and *tert*-leucine (**12**)] were synthesized, and their structures were analyzed with X-ray diffraction and CD spectral measurements. Variable temperature ^{1}H NMR measurements were performed to determine their equilibrium constants and their thermodynamic parameters. The use of two reference peptides made these quantitative studies possible. T3ASC, which contains three thiazole rings as a result of replacing oxazoline^2 with thiazole, and *d*ASC, in which the two oxazoline rings were deleted, were respectively used as square and folded reference peptides. The estimated parameters enabled more detailed discussion of the relationship between the bulkiness of substituents and the conformational free energies ($\Delta G°$) of the peptides as well as the relationship between structure and cytotoxicity. The $\Delta G°$ values for peptides **1**, **2**, **3**, **8**, **9** and **11** decreased with decreases in the bulkiness of their substituents. We suggest that spontaneous folding is promoted as the bulkiness of substituents decreases. Peptides **7** and **12**, which have large positive $\Delta G°$ values independently of temperature, did not exhibit spontaneous folding at any temperature; that is, their conformations were very stable in the square form. Peptides **4**, **5**, **6** and **10** had negative $\Delta G°$ values, despite their bulky substituents. Peptides with a positive $\Delta G°$ value showed cytotoxicity, and peptides with a negative $\Delta G°$ value showed reduced or no cytotoxicity. However, peptides **5** and **6** showed cytotoxicity equal to or stronger than **1**. Those ten peptides except for **5** and **6** showed a clear structure–cytotoxicity relationship based on $\Delta G°$ values.

Introduction

Ascidiacyclamide (**1**) is a cytotoxic cyclic peptide isolated from the marine invertebrate ascidian.[1] Peptide **1** has a C_2-symmetric sequence cyclo(-Ile^1-Oxz^2-D-Val^3-Thz^4-Ile^5-Oxz^6-D-Val^7-Thz^8-) containing the unusual amino acids (4S, 5R)-5-methyl-oxazoline-4-carboxylic acid (Oxz) and thiazole-4-carboxylic acid (Thz) (Fig. 1). Previous structural analyses revealed that **1** assumes two major conformations: a "square form" in which the Oxz and Thz rings are located at the four corners of the open peptide backbone, and a "folded form" in which the peptide backbone is folded at around the two Oxz rings and the Thz rings face each other.[2–4] In solution, peptide **1** is in an equilibrium between the square and folded conformations (Fig. 2).[5] We have also introduced asymmetric modifications in which the Ile^1 residue was replaced with other amino acids [Xxx^1: Ala (**2**), Val (**3**), Leu (**4**), Phe (**5**), cyclohexylalanine (Cha) (**6**) and phenylglycine (Phg) (**7**)][6–9] (Fig. 1). These modifications showed that the repulsive steric interactions between the side chains of the Xxx^1 and Ile^5 residues, which are close to one another within the square form, contribute to the conformational equilibrium between the square and folded conformers, and are related to their cytotoxicity.[6–10]

In 1955, the A values of substituent as the free energy difference between the axial and equatorial isomers of mono-substituted cyclohexanes were defined by Winstein and Holness.[11] The equatorial isomer becomes predominant as the corresponding size of substituent grows, and the A values

Osaka University of Pharmaceutical Sciences, 4-20-1 Nasahara, Takatsuki, Osaka 569-1094, Japan. E-mail: asano@gly.oups.ac.jp; Fax: +81-72-690-1005; Tel: +81-72-690-1066
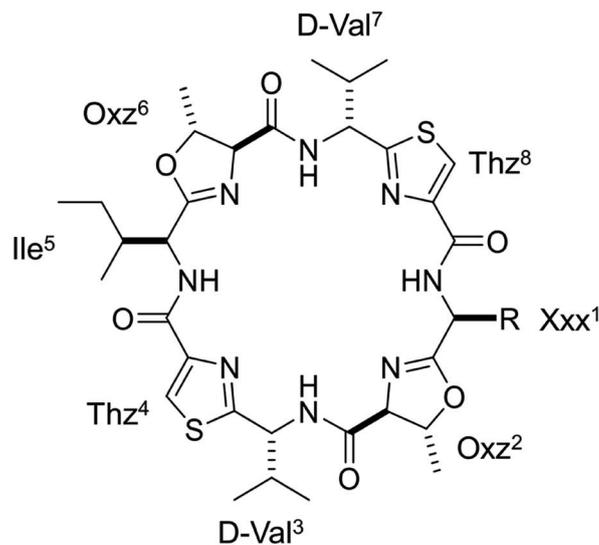
Ascidiacyclamide

Peptide	1	2	3	4	5	6
Xxx[1]	Ile	Ala	Val	Leu	Phe	Cha
R						
Peptide	7	8	9	10	11	12
Xxx[1]	Phg	Abu	Nva	Tbu	Chg	Tle
R						

Fig. 1   Chemical structures of 1 and the side chains (R) of the Xxx[1] residues in the asymmetric analogues (2–12). Peptides 1–7 are the previously synthesized.[2–9] Peptides 8–12 are new asymmetric analogues.
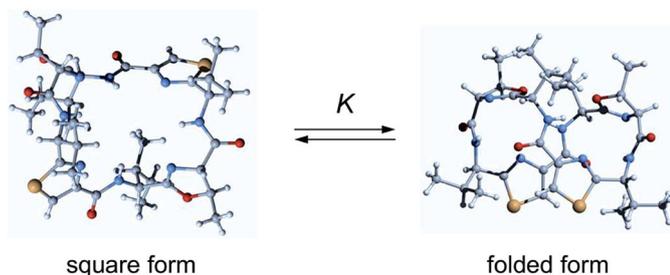

Fig. 2   Conformational equilibrium of ascidiacyclamides between the square and folded forms.

increase concomitantly. This parameter is a very useful resource to assess the steric size of variety of substituents. Many other conformational analyses using cyclohexane and its analogues have been carried out in an effort to understand steric repulsion within a molecule.[12–17] We were interested in assessing the conformational equilibrium quantitatively to better understand the conformational behavior of ascidiacyclamides. In order to determine the equilibrium constants experimentally, it is necessary to observe an independent signal from each conformer. However, the signals from a small peptide like ascidiacyclamides equilibrate rapidly between the two conformers on the NMR time scale. It is often possible to slow down the equilibration of the signals by measuring at low temperatures, but in the case of ascidiacyclamides, the signals
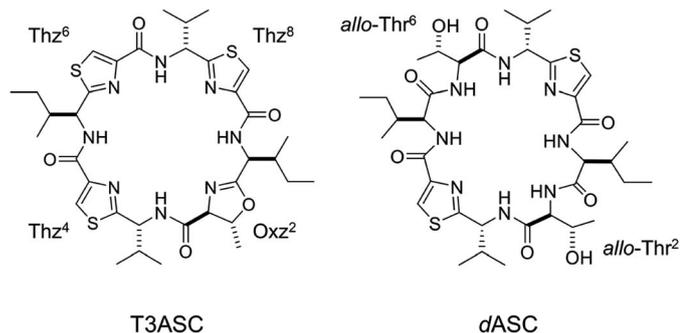
Fig. 3   Chemical structures of T3ASC and dASC.

corresponding to the two conformers were still not separated when the temperature was lowered to −60 °C in acetonitrile-d_3 solution. To overcome this limitation with small peptides, NMR-based quantitative studies of β-sheet populations have been carried out using reference peptides for the folded and unfolded states.[18,19] For instance, to determine the β-sheet populations of flexible linear peptides, disulfide-linked cyclic peptides (or backbone cyclization) and residue truncated peptides were used as controls to provide reference chemical

shifts for the fully folded and random coil states, respectively. We therefore searched for square and folded reference peptides to apply this strategy to ascidiacyclamides. The results showed that the T3ASC and dASC analogues were potential models for the fully square and folded states, respectively (Fig. 3). T3ASC, cyclo(-Ile[1]-Thz[2]-D-Val[3]-Thz[4]-Ile[5]-Oxz[6]-D-Val[7]-Thz[8]-) contains three Thz rings, as the Oxz[2] ring was replaced with a Thz[2] ring. The crystal structure of T3ASC exhibited a square form very similar to that of **1** (The RMS deviation = 0.351 Å) (Fig. S43†), and most T3ASC molecules reportedly retain the square form even in solution.[20] On the other hand, dASC, cyclo(-Ile-alloThr-D-Val-Thz-)₂, which lacks the Oxz rings of **1**, assumes a folded form in both solid and solution states (Fig. S44†).[21] Asymmetric modifications were also made in dASC, but unlike **1**, all dASC analogues were folded, regardless of the bulkiness of the side chain of the replaced amino acid. The folded conformation of dASC was stabilized by four intramolecular hydrogen bonds, making it unable to transform to the square form from the folded form, and it exhibited no cytotoxicity.[21,22]

In the present study, five new asymmetric acidiacyclamide analogues [Xxx[1]: 2-aminobutyric acid (Abu) (**8**), 2-aminopentyric acid (Nva) (**9**), tert-butylalanine (Tbu) (**10**), cyclohexylglycine (Chg)
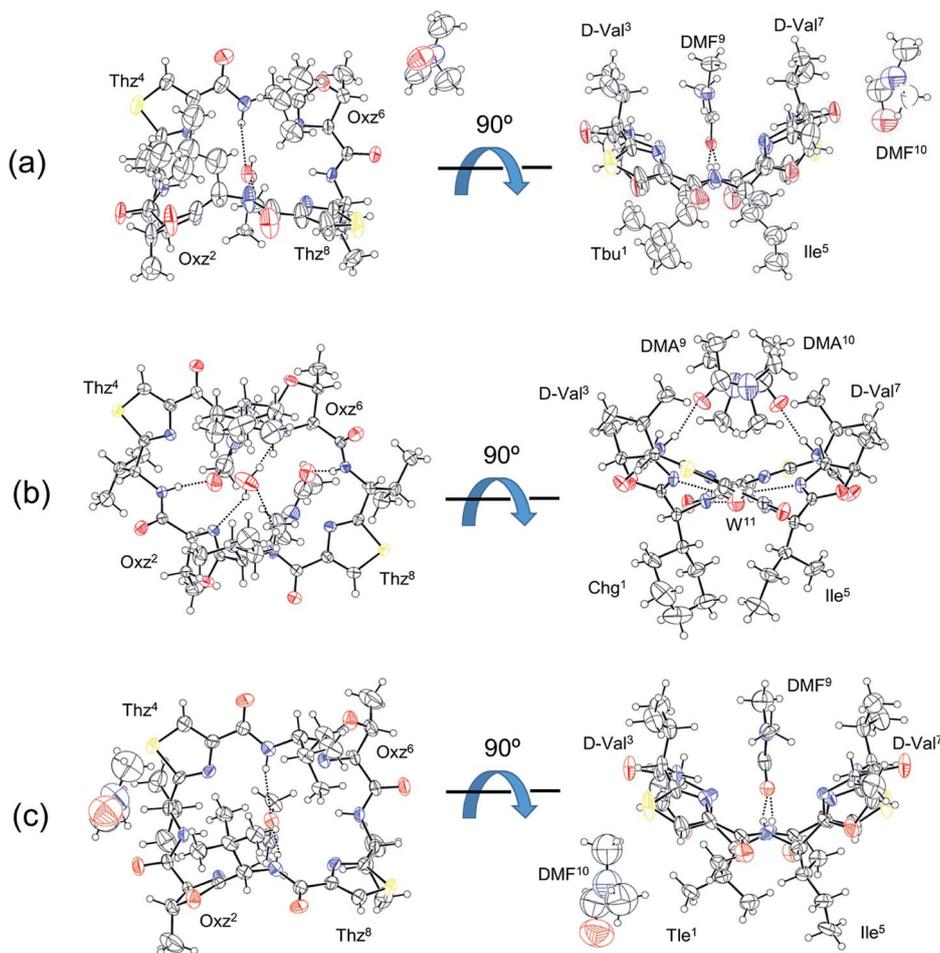

Fig. 4   Crystal structures of peptides **10**, **11** and **12** are shown in (a), (b) and (c), respectively. Shown are top (left) and side (right) views of the peptide rings. The dashed lines represent hydrogen bonds.

(**11**) and *tert*-leucine (Tle) (**12**)] were synthesized (Fig. 1). We first describe their structural characterization using X-ray diffraction and circular dichroism (CD) spectroscopy, and then discuss the NMR-based quantification of the conformational equilibrium for **1** and eleven asymmetric analogues (the aforementioned six analogues, **2–7**, and five new analogues, **8–12**).

Results and discussion

Crystal structures

Three of the new five asymmetric analogues, **10**, **11** and **12**, were crystallized (Fig. 4). Crystals of **10** and **12** were grown in dimethylformamide (DMF) solution. With their crystal structures, each asymmetric unit contained the peptide molecule and two DMF molecules. Each peptide backbone was open, and a DMF molecule was held at the center of the cyclic peptide with two hydrogen bonds: $N(Xxx^1)–H\cdots O(DMF)$ and $N(Ile^5)–H\cdots O(DMF)$. The distances and angles of these hydrogen bonds are listed in Table 1. The second DMF molecule was not involved in hydrogen bonding. Peptide **11** was crystallized in a dimethylacetamide (DMA) and water solvent mixture. Within its crystal structure, the asymmetric unit contained the peptide molecule, two DMA molecules and a water molecule. The peptide backbone was open, and a water and two DMA molecules were held at the center of cyclic peptide by a hydrogen bonding network (Fig. 4, Table 1).

We have been using the diagonal distance between the nitrogen atoms of the two Oxz and Thz rings ($N(Oxz^2)\cdots N(Oxz^6)$ and $N(Thz^4)\cdots N(Thz^8)$) as an index to characterize the square form in crystal.[2,7–9] These distances in the crystals of **10**, **11** and **12** are listed together with the previously collected data for **1** in Table 2. Whereas the diagonal distances in **10** and **12** are similar to that in **1**, the $N(Oxz^2)\cdots N(Oxz^6)$ distance is shorter and the $N(Thz^4)\cdots N(Thz^8)$ distance is longer in **11** than in **1**. Thus, **10** and **12** were classified as being in the original square form, while **11** exhibited different diagonal distances but was open. In previous X-ray analyses, the crystal structures of **2** and **5** were classified as being in the folded form,[6,7] and the crystal

Table 1 Hydrogen bonds in the crystal structures of **10**, **11** and **12**[a]

Peptide	Donor D–H	Acceptor A	Distance (Å) D⋯A	Angle (°) D–H⋯A
10	$N(Tbu^1)–H$	$O(DMF^9)$	3.104(2)	163.2
	$N(Ile^5)–H$	$O(DMF^{10})$	2.928(2)	163.7
11	$N(Chg^1)–H$	W	3.262(7)	137.3
	$N(D\text{-}Val^3)–H$	$O(DMA^9)$	2.904(6)	169.2
	$N(Ile^5)–H$	W	3.247(7)	137.5
	$N(D\text{-}Val^7)–H$	$O(DMA^{10})$	2.916(6)	168.3
	W–H	$N(Oxz^2)$	2.835(7)	165.5
	W–H	$N(Oxz^6)$	2.831(7)	137.9
12	$N(Tle^1)–H$	$O(DMF^9)$	3.161(6)	167.4
	$N(Ile^5)–H$	$O(DMF^{10})$	3.161(6)	167.4

[a] A letter of W represents the oxygen atom of water.

Table 2 Comparison of selected nonbonding distances (Å) between the nitrogen atoms of the five-membered rings in **1**, **10**, **11** and **12**

Peptide	$N(Oxz^2)\cdots N(Oxz^6)$	$N(Thz^4)\cdots N(Thz^8)$
1[a]	6.46	6.40
10	6.53	6.60
11	5.39	8.07
12	6.65	6.53

[a] The square structure of **1** (benzene solvated) was previously reported.[2]

structures of **1**, **3**, **4**, **6** and **7** were classified as being in the square form.[2,7–9]

CD spectra

The CD spectral changes for the five new peptides, **8–12**, were measured in acetonitrile (CH_3CN) during titration of 2,2,2-trifluoroethanol (TFE) (Fig. 5). We have well established that measuring the CD spectral changes in this solvent system is a useful means of monitoring the conformational equilibrium between the square and folded forms of ascidiacyclamides.[7–9,20] Previously recorded CD spectra for **1** are also shown in Fig. 5. A positive band at about 205 nm and a small negative band at 245 nm in CH_3CN solution (bold line) are characteristic of the square form. TFE titration led to a decrease in $[\theta]_{205}$ and an increase in $[\theta]_{245}$, and a moderate positive band in the range of 230–260 nm was recorded in 100% TFE solution (dashed line). These spectral features are characteristic of the folded form. Moreover, the presence of a single isodichroic point at around 230 nm suggests conformational equilibrium.

The spectral changes observed with **11** showed the same features as **1** in this solvent system. The conformation of **11** in CH_3CN solution was the square form, which was converted to the folded form through TFE titration. The spectra for **3** had similar features.[7] The spectrum of **12** in CH_3CN solution had the same shape as that of **1**, but the spectral changes elicited by TFE titration were very small and were very similar to those of **7**.[9] The spectrum of **10** exhibited the features of the folded form, even in CH_3CN solution, and TFE titration elicited little change. The spectra of **2**, **4**, **5** and **6** have also been exhibited folded form.[7,8] In crystal, however, **2** and **5** were in the folded form, while **4**, **6** and **10** assumed the square form. The spectral features of **8** and **9** were very similar to each other. They did not exhibit a clear negative band around 245 nm in CH_3CN solution, as **1** did, but a single isodichroic point at around 230 nm was observed. Previously recorded CD spectra for **2–7** are shown in Fig. S41.†

We also evaluated the temperature dependencies of the CD spectra of ascidiacyclamides in CH_3CN solution at 273, 293, 313 and 333 K. The temperature dependencies of **1**, T3ASC, *d*ASC and **8–12** are shown in Fig. 6; those of peptides **2–7** are shown in Fig. S42.† The $[\theta]_{245}$ values decreased as temperature increased in all ascidiacyclamides spectra, except those of T3ASC, **7** and **12**. Peptides **1**, **3** and **11**, which exhibited a negative band at 245 nm at low temperature, showed a slight decrease in $[\theta]_{245}$
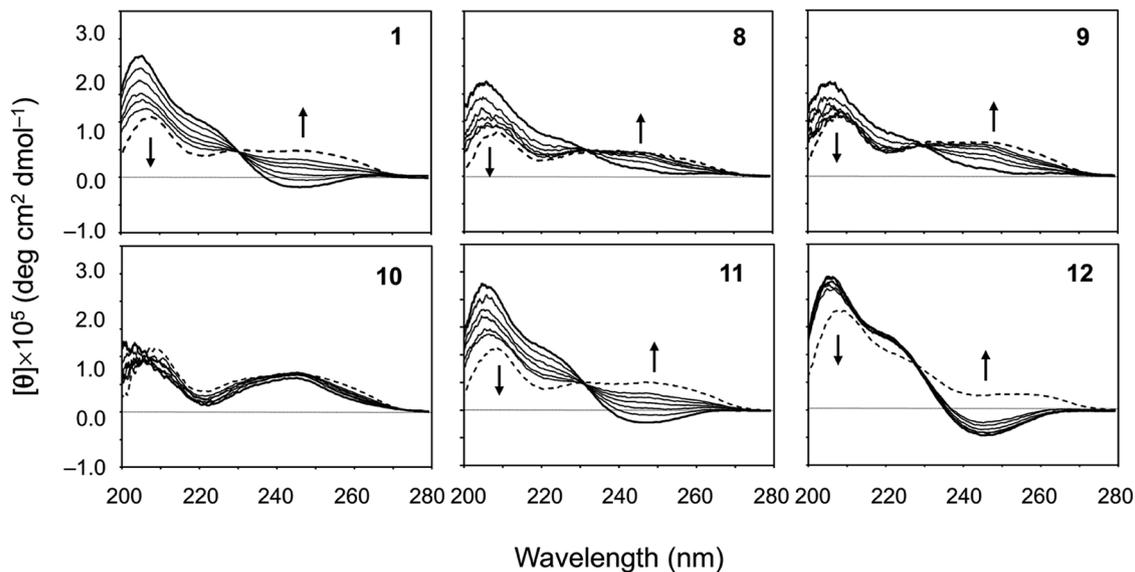
Fig. 5 CD spectral changes elicited by titration of TFE for peptides **1** and **8–12**. The CD spectra for **1** were taken from a previous report.[7] The spectra were measured in CH_3CN solution while changing the TFE concentration (10%, 20%, 30%, 40%, 50% and 100%). The spectra in 100% CH_3CN and 100% TFE solution are drawn in bold and dashed lines, respectively.

with increasing temperature. By contrast, peptides **2, 4, 5, 6, 8, 9** and **10** all showed strong temperature dependencies, with a positive band in the range of 230–260 at low temperature. In particular, a clear negative band at 245 nm appeared for **8** and **9** as the temperature increased. The spectrum of *d*ASC also showed a positive band in the range of 230–260 nm at low temperature. However, the decrease in $[\theta]_{245}$ with increasing temperature of *d*ASC was slight compared with these peptides.
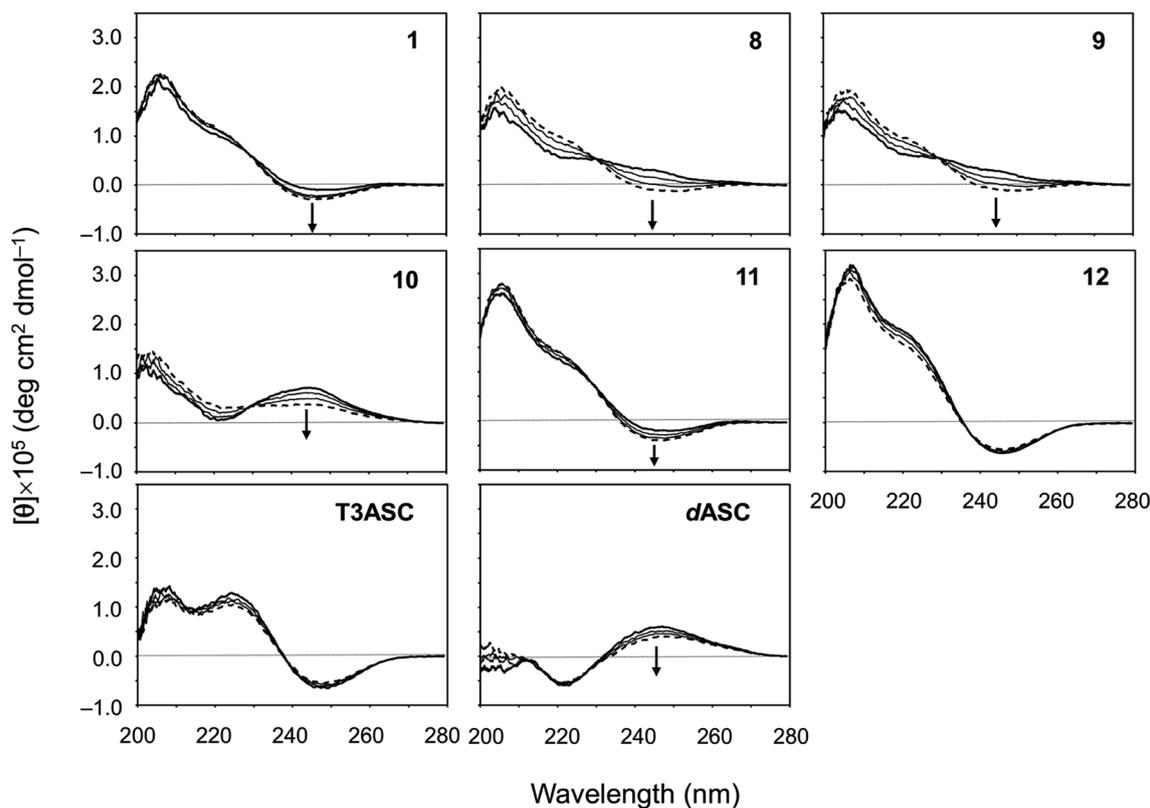

Fig. 6 Temperature dependence of the CD spectra of peptides **1, 8–12**, T3ASC and *d*ASC. The CD spectra for **1** are taken from a previous report.[29] The spectra were measured every 20 K in CH_3CN solution at 273–333 K. The CD spectra at 273 and 333 K are drawn in bold and dashed lines, respectively.

The spectra of T3ASC, **7** and **12** were little affected by increasing temperature. These observations suggest the following:

(1) The conformation of ascidiacyclamide changes from the folded form to the square form with increasing temperature.

(2) T3ASC, **7** and **12** in CH_3CN solution form the most stable square form against temperature increases.

(3) *d*ASC in CH_3CN solution forms the most stable folded form against temperature increases.

VT-^{1}H NMR

All ascidiacyclamides were examined using variable temperature ^{1}H NMR spectroscopy (VT-^{1}H NMR). The spectra were recorded every 10 K from 273 K to 333 K in CH_3CN-d_3 solution. The temperature coefficients ($\Delta\delta/\Delta T$ (ppb K^{-1})) of all amide and Thz protons are listed in Table 3. Although the temperature coefficients of **1–5** were reported previously,[7] we examined them again because different NMR equipment was used in the present study. In **1**, the chemical shifts of the amide protons of Ile[1,5] residues were shifted to lower fields with a temperature coefficient of 2.0 ppb K^{-1}, whereas the chemical shifts of the amide protons of D-Val[3,7] residues showed no temperature dependence. The temperature coefficients of all amide protons in **2–6** and **8–11** were positive, though they differed slightly among the 10 peptides. By contrast, none of the amide protons in T3ASC or **12** showed any temperature dependence, and the temperature coefficients of all amide protons in *d*ASC and **7** were negative. The behavior of the chemical shifts of amide protons elicited by temperature changes are generally discussed as a phenomenon caused by perturbation of intra/intermolecular hydrogen bonds, exposure to the solvent or shielding from the solvent,[23] but it is difficult to clearly conclude that from the present results. On the other hand, the behavior of

the chemical shifts of Thz protons can be clearly explained. When the Thz rings face each other in the folded form, the chemical shifts of the Thz[4] and Thz[8] protons appear in a higher field than those in the square form due to the ring-current effects of the Thz[8] and Thz[4] rings, respectively. In other words, the chemical shifts of Thz protons are very sensitive to backbone conformational changes. The temperature coefficients of the Thz protons were positive in *d*ASC, **1–6** and **8–11**. These observations suggest that the conformation of ASCs change from the folded form to the square form with increasing temperature. The Thz protons in T3ASC, **7** and **12** exhibited no temperature dependence. The temperature coefficients of the Thz protons of *d*ASC were not zero, but their temperature dependence was the lowest. There was thus good agreement between the temperature dependencies of the Thz protons chemical shifts and CD spectral changes.

NMR-based quantification of the conformational equilibrium

The conformational equilibrium constants (K) (Fig. 2) of ascidiacyclamides were determined using data from VT-^{1}H NMR studies in CH_3CN-d_3 solution. Based on structural analyses, T3ASC and *d*ASC were used as reference peptides to provide reference chemical shifts for the fully square and folded forms, respectively. K can be estimated for ascidiacyclamides from conformationally sensitive proton chemical shifts *via* eqn (1), where δ_{obs} is the chemical shift of the Thz proton within the equilibrating peptide, δ_S (= 8.09 ppm) is the chemical shift of the Thz proton in the fully square form (T3ASC), and δ_F (=7.35 ppm) is the chemical shift of the Thz proton in the fully folded form (*d*ASC). The chemical shift of the Thz proton in *d*ASC moved slightly to a lower field with increasing temperature, so the chemical shift at the lowest temperature (273 K) was used as the δ_F value.

$$K = (\delta_S - \delta_{obs})/(\delta_{obs} - \delta_F) \qquad (1)$$

For **1–12**, values of K and the Gibbs free energy ($\Delta G°$) were measured every 10 K from 237 K to 333 K (Tables S30, S32, S34, S36, S38, S40, S42, S44, S46, S48, S50 and S51†). In addition, $\Delta G°$ at 298 K was estimated from the thermodynamic parameters of ascidiacyclamide and the asymmetric analogues. The enthalpy ($\Delta H°$) and entropy ($\Delta S°$) were determined through a linear van't Hoff plot (ln K *versus* $1/T$), and then $\Delta G°$ at 298 K was calculated from eqn (2). For **7** and **12**, we could not obtain their values of $\Delta H°$ and $\Delta S°$ by a van't Hoff plot because their K values showed no temperature dependencies.

$$\Delta G° = \Delta H° - T\Delta S° = -RT \ln K \qquad (2)$$

These values are listed in Table 4. Folding of ascidiacyclamides was enthalpically favorable and entropically unfavorable. This thermodynamic profile is considered reasonable because four hydrogen bonds are formed by folding: $N(Xxx^1)H\cdots O^\gamma(Oxz^6)$, $N(D\text{-}Val^3)H\cdots O(Thz^8)$, $N(Ile^5)H\cdots O^\gamma(Oxz^2)$ and $N(D\text{-}Val^7)H\cdots O(Thz^4)$. The average values of $\Delta H°$ and $\Delta S°$ were respectively determined to be -13.55 (2.06) kJ mol^{-1} and -43.72 (4.71) J K^{-1} mol^{-1}, and there were no significant

Table 3 Amide proton and Thz proton temperature coefficients $\Delta\delta/\Delta T$ (ppb K^{-1}) of peptides **1–12**, T3ASC and *d*ASC in CH_3CN-d_3 solution

Peptide	Xxx[1]NH	D-Val[3]NH	Ile[5]NH	D-Val[7]NH	ThzH[a]	ThzH[a]
1[b]	2.0	0.0	2.0	0.0	1.9	1.9
2[b]	2.0	1.6	2.2	1.0	3.9	3.9
3[b]	2.3	0.6	2.9	0.9	2.9	3.1
4[b]	1.9	0.7	2.4	1.5	3.3	3.3
5[b]	1.1	0.7	2.1	1.0	3.5	3.2
6	2.0	0.9	2.5	1.5	3.5	3.5
7	—[d]	−2.2	−0.7	−1.4	0.0	—[d]
8	2.2	—[d]	2.7	1.0	3.3	3.3
9	2.0	—[d,e]	2.5	0.9[e]	3.0	3.2
10	—[d]	0.6	2.0	1.4	2.5	2.7
11	2.5	—[d,e]	2.1	0.5[e]	2.0	2.0
12	0.0	—[d]	0.0	—[d]	0.0	0.0
T3ASC	0.0	—[d]	0.0	—[d]	0.0	0.0
*d*ASC[c]	−1.1	−1.3	−1.1	−1.3	1.3	1.3

[a] The chemical shifts of Thz[4]H and Thz[8]H were indistinguishable. [b] The temperature coefficients of these peptides have already been reported.[7] However, they were measured again because different NMR equipment was used in this study. [c] *d*ASC also includes *allo*-Thr[2]NH and *allo*-Thr[6]NH. The temperature coefficient for both was −2.3 ppb K^{-1}. [d] The correlation coefficients were less than 0.9. [e] The chemical shifts of D-Val[3]NH and D-Val[7]NH were indistinguishable.

Table 4 Thermodynamic parameters of peptides **1–12**

Peptide	ΔH° (kJ mol^{-1})	ΔS° (J K^{-1} mol^{-1})	$\Delta G^\circ_{298\ \mathrm{K}}$ (kg mol^{-1})
1[a]	−9.55	−39.40	2.19
2[a]	−16.76	−52.29	−1.03
3[a,b]	−13.60	−49.00	1.00
4[a]	−14.83	−44.67	−1.52
5[a,b]	−15.80	−47.50	−1.64
6[a]	−15.80	−47.60	−1.62
7[c]	—	—	4.32
8[a]	−13.83	−45.23	−0.35
9[a,b]	−13.23	−44.18	−0.06
10[a,b]	−14.14	−38.59	−2.64
11[a]	−9.85	−39.55	1.93
12[c]	—	—	4.91

[a] ΔH° and ΔS° values were determined from the linear fitting to the van't Hoff equation. [b] Since the chemical shifts of Thz^{4}H and Thz^{8}H were observed separately, these parameters were determined in duplicate. The values with the larger correlation coefficient are given here. [c] The temperature dependence of the equilibrium constant (K) is not shown. The $\Delta G^\circ_{298\ \mathrm{K}}$ value was calculated from $\Delta G^\circ = -RT \ln K$.

differences in these values among ascidiacyclamides. The ΔG° values for both **7** and **12** were positive and very large, which means that the conformational equilibrium positions of **7** and **12** are significantly shifted in the opposite direction. As shown in Fig. 7, within the measured temperature range, the ΔG° values for **1** and **11** are positive at every temperature, suggesting that there is no spontaneous folding. The ΔG° values for **3** are positive at higher temperatures but negative below 278 K. Peptides **8** and **9** will fold spontaneously at temperatures below 303 K. Peptides **4**, **5** and **6** will fold spontaneously at temperatures below 333 K, and the ΔG° values are near zero at around 333 K. Peptide **10** appears to spontaneously fold at any temperature.

The ΔG° values at 298 K for all ascidiacyclamides are arranged in descending order in Fig. 8. These results allow for a logical discussion that takes into account the counterpoise
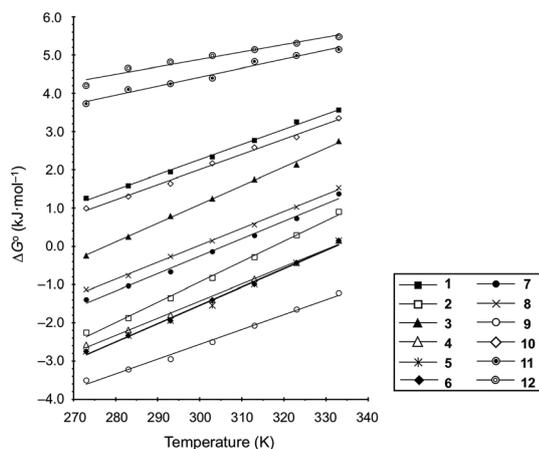

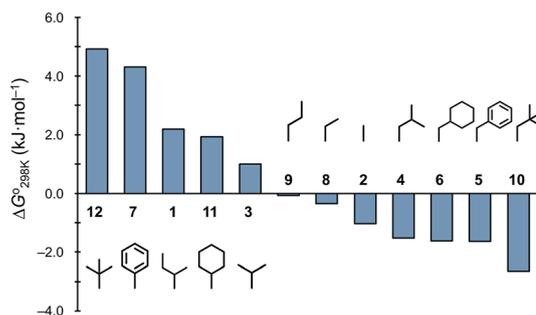**Fig. 7** Plots of the temperature dependences of the free energies for peptides **1–12**.

Fig. 8 Plots of the free energies for peptides **1–12** at 298 K in descending order. The chemical structures in the figure are the side chains of the Xxx^1 residues.

between the bulkiness of substituents in the Xxx^1 and Ile^5 residues. Symmetric peptide (**1**) showed a preference for the square form in CH$_3$CN-d_3 solution at 298 K, with a ΔG° value of 2.19 kJ mol^{-1}, while **11**, which contains a cyclohexyl group, had nearly the same ΔG° value as **1**. Comparison among peptides **1**, **2**, **3**, **8** and **9** revealed that the ΔG° value decreased with a decrease in the carbon number of the substituent. In addition, although peptides **3** and **9** have the same number of carbon atoms in their side chains, the ΔG° value was smaller for **9**, which has a linear alkyl group, than for **3**, which has a branched alkyl group (*sec*-butyl (**1**) > isopropyl (**3**) > *n*-propyl (**9**) > ethyl (**8**) > methyl (**2**)). The ΔG° value for **9** was nearly zero, and those of **2** and **8** were negative, indicating a preference for the folded form. In the square form, the side chain of the Xxx^1 residue is close to the *sec*-butyl group of the Ile^5 residue, and we suggest that the attractive force between these two functional groups is greater than the repulsive force. Consequently, with a decrease in the bulkiness of the substituent in the Xxx^1 residue, the attractive force will be weakened, and the peptide will be easier to fold. Peptides **4**, **5**, **6** and **10** had even greater preferences for the folded form. The ΔG° value for **10** was −2.64 kJ mol^{-1}, which was the minimum value, but those of **4**, **5** and **6** were nearly the same. The common feature for the substituents of **4**, **5**, **6** and **10** is a β-methylene. This spacer may reduce contacts between the Xxx^1 and Ile^5 residues within these peptides. By contrast, peptides **7** and **12** had strong preferences for the square form. Although the *tert*-butyl group (**12**) and *sec*-butyl group (**1**) are both four carbon alkyl groups, the former is branched and therefore may exert a greater dispersion force. While it is apparent that the van der Waals space occupied by a cyclohexyl group (**11**) is larger than that occupied by a planarity phenyl group (**7**), the ΔG° for **7** was nevertheless significantly greater than that for **11**. A dispersion force like the CH–π interaction may be acting between the phenyl group of the Phg^1 residue and *sec*-butyl group of the Ile^5 residue. The additional attractive force may increase the stability of the square form, though that could not be verified here. Still, the very high stabilities of square forms of **7** and **12** are noteworthy.

Structure–cytotoxicity relationship

We assessed the cytotoxicity of the five new peptides, **8–12**, by determining the ED$_{50}$ against P388 mouse lymphocytic

Table 5 Summary of cytotoxicities and structures of peptides **1–12**, T3ASC and *d*ASC

Peptide	ED_{50} (µg mL^{-1})	Structure in solid	Structure in solution
1	10.5[a]	Square[b]	$\Delta G^{\circ}_{298\ \mathrm{K}} > 0$
2	49.0[a]	Folded[a]	$\Delta G^{\circ}_{298\ \mathrm{K}} < 0$
3	7.4[a]	Square[a]	$\Delta G^{\circ}_{298\ \mathrm{K}} > 0$
4	29.5[a]	Square[c]	$\Delta G^{\circ}_{298\ \mathrm{K}} < 0$
5	11.8[a]	Folded[a]	$\Delta G^{\circ}_{298\ \mathrm{K}} < 0$
6	5.6[d]	Square[d]	$\Delta G^{\circ}_{298\ \mathrm{K}} < 0$
7	12.4[e]	Square[e]	$\Delta G^{\circ}_{298\ \mathrm{K}} > 0$
8	>100	—[f]	$\Delta G^{\circ}_{298\ \mathrm{K}} < 0$
9	18.7	—[f]	$\Delta G^{\circ}_{298\ \mathrm{K}} \approx 0$
10	>100	Square	$\Delta G^{\circ}_{298\ \mathrm{K}} < 0$
11	3.4	Square	$\Delta G^{\circ}_{298\ \mathrm{K}} > 0$
12	5.5	Square	$\Delta G^{\circ}_{298\ \mathrm{K}} > 0$
T3ASC	0.93[g]	Square[g]	—
*d*ASC	>100[h]	Folded[i]	—

[a] These are taken from a previous report.[7] [b] This datum is taken from a previous report.[2] [c] This datum is taken from a previous report.[6] [d] These data are taken from a previous report.[8] [e] These data are taken from a previous report.[9] [f] These crystal structures have not obtained yet. [g] These data are taken from a previous report.[20] [h] This datum is taken from a previous report.[22] [i] This datum is taken from a previous report.[21]

leukemia cells. Our findings, including data collected previously, are summarized in Table 5 with their structures. Peptides **3**, **7**, **11** and **12**, which have the same conformation as the parent peptide (**1**) in both the crystal and solution, showed cytotoxicity equivalent to or stronger than peptide **1**. Peptide **9**, with a ΔG°_{298} value close to zero, exhibited half the cytotoxicity of **1**, while peptides **2** and **8**, with negative ΔG°_{298} values, showed one-fifth the cytotoxicity and no cytotoxicity, respectively. These results suggest that a structural change from the square to the folded form decreases the cytotoxicity. Consistent with those ideas, the reference peptide for the square form (T3ASC) showed the strongest cytotoxicity, while the reference for the folded form (*d*ASC) showed no cytotoxicity. Peptides **4**, **5**, **6** and **10** all had negative ΔG° values. The cytotoxicity of **4** was reduced to one-third that of **1**, and **10** showed no cytotoxicity. One the other hand, peptides **5** and **6** showed cytotoxicity equal to or stronger than **1**. Thus, peptides **5** and **6** did not adhere to the structure–cytotoxicity relationship observed with the others.

Conclusions

NMR-based experiments making use of two reference peptides (T3ASC and *d*ASC) enabled highly precise determination of equilibrium constants and then thermodynamic parameters (ΔG°, ΔH° and ΔS°). For peptides **1**, **2**, **3**, **8**, **9** and **11**, there was a correlation between the bulkiness of their substituents and their ΔG° value. This suggests that the dispersion force between the substituent in the Xxx^1 residue and *sec*-butyl group of the Ile^5 residue contributed to the stabilization of the square form. Peptides **7** and **12** showed large ΔG° values independently of

temperature. This suggests the stability of the square forms of **7** and **12** may involve other factors in addition to the dispersive force. Peptides **4**, **5**, **6** and **10** had negative ΔG° values, despite of their bulky substituents. The β-methylene bearing on substituents may weaken the dispersion force between the side chains of Xxx^1 and Ile^5 residues. However, the crystal structures of these peptides were square form, except for **5**. Considering the structure–cytotoxicity relationship based on the estimated ΔG° values, good correlation was exhibited for ten peptides except for **5** and **6**. The estimated parameters in the present study allowed for a more detailed discussion of the ascidiacyclamide conformational equilibrium.

Experimental

Synthesis

First, the Thz unit (Boc-D-Val(Thz)-OMe) was synthesized as previously described.[24,25] Peptides were synthesized using a conventional liquid-phase method. The linear peptide Boc-Xxx-*allo*-Thr-D-Val-Thz-Ile-*allo*-Thr-D-Val-Thz-OMe was synthesized using 1-hydroxybenzotiazole (Watanabe Chemical lnd. Ltd., Hiroshima, Japan) and 1-ethyl-3-(3-dimethylaminopropyl) carbodiimide hydrochloride (Watanabe Chemical lnd. Ltd., Hiroshima, Japan). Then, macro-cyclization to cyclo(-Xxx-*allo*-Thr-D-Val-Thz-Ile-*allo*-Thr-D-Val-Thz-) was accomplished using benzotriazolyloxy-tris (pyrrolidino)-phosphonium hexafluorophosphate (Watanabe Chemical lnd. Ltd., Hiroshima, Japan) in the presence of 4-dimethylaminopyridine (Nacalai Tesque, Kyoto, Japan). Thereafter, the Oxz rings were formed by reacting the Ile-*allo*-Thr moieties with bis(2-methoxyethyl) aminosulfur trifluoride (Deoxo-Fluor) (Fujifilm Wako Pure Chemical Corp., Osaka, Japan).[26] The synthesis and characterization of **8–12** are detailed in ESI.†

^{1}H NMR spectra

^{1}H NMR spectra were recorded on an Agilent DD2 600 MHz NMR spectrometer (Agilent Technologies, California, USA). Peptide concentrations were about 5.0 mM in CH$_3$CN-d_3. Chemical shifts were measured relative to internal trimethylsilane at 0.00 ppm. The protons were assigned using two dimensional correlated spectroscopy (2D-COSY) and rotating-frame Overhauser effect spectroscopy (ROESY; mixing time = 500 ms). The assignment lists and ^{1}H NMR spectra for all peptides are given in ESI.†

X-ray diffraction

Peptides **10** and **12** were crystallized in DMF, and peptide **11** was crystallized in DMA. X-ray diffraction data for **10** were collected with a Rigaku CrysAlis Pro (Rigaku Corp., Tokyo, Japan). The structure was solved using SHELXT[27] and refined using SHELXL2016/4.[28] X-ray diffraction data for **11** and **12** were collected with a Bruker Smart APEXII (Bruker Corp., Massachusetts, USA). The structures were solved using SHELX-97 (ref. 29) and refined using SHELXL-97.[29] The crystal data for **10**, **11** and **12** have been deposited with the Cambridge Crystallographic Data Center under deposition numbers 2007056,

2007057 and 2007058,† respectively. The crystal data for these three peptides are given in ESI.†

CD spectra

The CD spectra were measured using a JASCO spectrapolarimeter J-820 (JASCO ltd., Tokyo, Japan). The peptide concentrations were about 0.04 mM in CH_3CN solution, and the path length was 1 cm. The experiments with TFE titration were performed at room temperature. The temperature dependencies of the CD spectra were measured at 273, 293, 313 and 333 K. The spectra were scanned at a speed of 5 nm min^{-1} with 0.1 nm interval uptake to a computer. Data were averaged over each 1 nm and plotted.

Assay for cytotoxicity

The cytotoxicity of the peptides was assessed using the 3-(4,5-dimethyl-2-thiazolyl)-2,5-diphenyl-2H-tetrazolium bromide (MTT) method as described previously with some modifications.[30,31] 388 mouse lymphocytic leukemia cells were cultured in RPMI 1640 medium (10% fetal calf serum) at 37 °C under 5% CO_2. The test materials were dissolved in dimethyl sulfoxide (DMSO) to a concentration of 10 mM, and the solution was diluted with Essential Medium to concentrations of 200, 20, and 2 μM, respectively. Each solution was combined with cells suspended (1×10^5 cells per mL) in the same medium. After incubating at 37 °C for 72 h under 5% CO_2, the cells were labeled with 5 mg mL^{-1} MTT in phosphate-buffered saline (PBS), and the absorbance of formazan dissolved in 20% sodium dodecyl sulfate (SDS) in 0.1 N HCl was measured at 540 nm with a microplate reader MTP-310 (Corona electric Co. Ltd, Hitachinaka, Japan). The absorbance values were expressed as percentages relative to that of the control cell suspension that was prepared using the same procedure described above but without a test substance. All assays were performed three times, semilogarithmic plots were constructed from the averaged data, and the effective dose of a substance required to inhibit cell growth by 50% (ED_{50}) was determined.

Conflicts of interest

There are no conflicts to declare.

References

1 Y. Hamamoto, M. Endo, M. Nakagawa, T. Nakanishi and K. Mizukawa, *Chem. Commun.*, 1983, 323–324.

2 T. Ishida, M. Inoue, Y. Hamada, S. Kato and T. Shioiri, *Chem. Commun.*, 1987, 370–371.

3 T. Ishida, Y. In, M. Inoue, Y. Hamada and T. Shioiri, *Biopolymers*, 1992, **32**, 131–143.

4 Y. In, M. Doi, M. Inoue, Y. Hamada and T. Shioiri, *Chem. Pharm. Bull.*, 1993, **41**, 1686–1690.

5 T. Ishida, M. Tanaka, M. Nabae, M. Inoue, S. Kato, Y. Hamada and T. Shioiri, *J. Org. Chem.*, 1988, **53**, 107–112.

6 M. Doi, F. Shinozaki, Y. In, T. Ishida, D. Yamamoto, M. Kamigauchi, M. Sugiura, Y. Hamada, K. Kohda and T. Shioiri, *Biopolymers*, 1999, **49**, 459–469.

7 A. Asano, K. Minoura, T. Yamada, A. Numata, T. Ishida, Y. Katsuya, Y. Mezaki, M. Sasaki, T. Taniguchi, M. Nakai, H. Hasegawa, A. Terashima and M. Doi, *J. Pept. Res.*, 2002, **60**, 10–22.

8 A. Asano, T. Yamada, A. Numata and M. Doi, *Acta Crystallogr., Sect. C: Cryst. Struct. Commun.*, 2003, **59**, o488–o490.

9 A. Asano, T. Yamada and M. Doi, *Bioorg. Med. Chem.*, 2011, **19**, 3372–3377.

10 A. Asano, K. Minoura, T. Yamada and M. Doi, *J. Pept. Sci.*, 2016, **22**, 156–165.

11 E. L. Eliel, S. H. Wilen and L. N. Mander, *Stereochemistry of organic compounds*, Wily & Sons, New York, 1994.

12 E. L. Eliel, N. L. Allinger, S. J. Angyal and G. A. Morrison, *Conformational Analysis*, Wiley & Sons, New York, 1965.

13 (a) N. L. Allinger and J. Allinger, *J. Am. Chem. Soc.*, 1958, **80**, 5476–5480; (b) N. L. Allinger, J. Allinger, L. A. Freiberg, R. F. Czaja and N. A. LeBel, *J. Am. Chem. Soc.*, 1960, **82**, 5876–5882.

14 (a) N. L. Allinger and H. M. Blatter, *J. Am. Chem. Soc.*, 1961, **83**, 994–995; (b) N. L. Allinger and L. A. Freiberg, *J. Am. Chem. Soc.*, 1962, **84**, 2201–2203; (c) B. Rickborn, *J. Am. Chem. Soc.*, 1962, **84**, 2414–2417; (d) W. D. Cotterill and M. J. T. Robinson, *Tetrahedron*, 1964, **20**, 777–790.

15 (a) C. Djerassi, E. J. Warawa, J. M. Berdahl and E. J. Eisenbraun, *J. Am. Chem. Soc.*, 1961, **83**, 3334–3336; (b) W. D. Cotterill and M. J. T. Robinson, *Tetrahedron*, 1964, **20**, 765–775.

16 (a) O. Takahashi, K. Yamasaki, Y. Kohno, K. Ueda, H. Suezawa and M. Nishio, *Chem.–Asian J.*, 2006, **1**, 852–859; (b) O. Takahashi, K. Yamasaki, Y. Kohno, K. Ueda, Y. Umezawa, H. Suezawa and M. Nishio, *Tetrahedron*, 2008, **64**, 2433–2440.

17 (a) Y. Carcenac, P. Diter, C. Wakselman and M. Tordeux, *New J. Chem.*, 2006, **30**, 442–446; (b) Y. Carcenac, M. Tordeux, C. Wakselman and P. Diter, *New J. Chem.*, 2006, **30**, 447–457.

18 F. A. Syud, J. F. Espinosa and S. H. Gellman, *J. Am. Chem. Soc.*, 1999, **121**, 11577–11578.

19 C. D. Tatko and M. L. Waters, *J. Am. Chem. Soc.*, 2004, **126**, 2028–2034.

20 A. Asano, T. Yamada, T. Taniguchi, M. Sasaki, K. Yoza and M. Doi, *J. Pept. Sci.*, 2018, e3120.

21 A. Asano, M. Doi, K. Kobayashi, M. Arimoto, T. Ishida, Y. Katsuya, Y. Mezaki, H. Hasegawa, M. Nakai, M. Sasaki, T. Taniguchi and A. Terashima, *Biopolymers*, 2001, **58**, 295–304.

22 A. Asano, T. Yamada, Y. Katsuya, T. Taniguchi, M. Sasaki and M. Doi, *J. Pept. Res.*, 2006, **66**(suppl. 1), 90–98.

23 (a) M. Ohnishi and D. W. Urry, *Biochem. Biophys. Res. Commun.*, 1969, **36**, 194–202; (b) N. Sugawara, E. S. Stevens, G. M. Bonora and C. Tonioro, *J. Am. Chem. Soc.*, 1980, **102**, 7044–7047; (c) E. S. Stevens, N. Sugawara, G. M. Bonora and C. Tonioro, *J. Am. Chem. Soc.*, 1980, **102**, 7044–7047; (d) R. R. Wilkening, E. S. Stevens, G. M. Bonora

and C. Tonioro, *J. Am. Chem. Soc.*, 1983, **105**, 2560–2561; (*e*) G. M. Bonora, C. Mapelli, C. Toniolo, R. R. Wilkening and E. S. Stevens, *Int. J. Biol. Macromol.*, 1984, **6**, 179–188.

24 Y. Hamada, S. Kato and T. Shioiri, *Tetrahedron Lett.*, 1985, **26**, 3223–3226.

25 Y. Hamada, M. Shibata, T. Sugiura, S. Kato and T. Shioiri, *J. Org. Chem.*, 1987, **52**, 1252–1255.

26 A. J. Phillips, Y. Uto, P. Wipf, M. J. Reno and D. R. Williams, *Org. Lett.*, 2000, **2**, 1165–1168.

27 G. M. Sheldrick, *Acta Crystallogr., Sect. A: Found. Adv.*, 2015, **71**, 3–8.

28 G. M. Sheldrick, *Acta Crystallogr., Sect. C: Struct. Chem.*, 2015, **71**, 3–8.

29 G. M. Sheldrick, *Acta Crystallogr., Sect. A: Found. Crystallogr.*, 2008, **64**, 112–122.

30 K. Kohda, Y. Ohta, Y. Yokoyama, T. Kato, Y. Suzumura, Y. Hamada and T. Shioiri, *Biochem. Pharmacol.*, 1989, **38**, 4497–4500.

31 K. Kohda, Y. Ohta, Y. Kawazoe, T. Kato, Y. Suzumura, Y. Hamada and T. Shioiri, *Biochem. Pharmacol.*, 1989, **38**, 4500–4502.